Topological Entropy of One-Dimensional Maps: Approximations and Bounds

N. J. Balmforth and E. A. Spiegel
Department of Astronomy, Columbia University, New York, New York 10027

C. Tresser
IBM T.J. Watson Laboratories, Yorktown Heights, New York 10598
(Received 2 August 1993)

We present a method for computing the topological entropy of one-dimensional maps. As an approximation scheme, the algorithm converges rapidly and provides both upper and lower bounds.

PACS numbers: 47.20.Ky, 05.45.+b

The topological entropy of a dynamical system was introduced in the sixties as a quantity that is invariant under continuous changes of coordinates [1]. It has better continuity properties than other indicators of the degree of chaos, the Lyapunov exponents or the metric entropy, on which it is an upper bound. Further, the topological entropy is well suited to the theoretical description of the transition to chaos. For many families of maps, the transition to complex behavior is reflected in the topological entropy as a second-order phase transition [2] (see Figs. 1 and 2). Thus the topological entropy has figured increasingly in quantifications of chaos and discussions of the physical effects of chaos. In dynamo theory, for example, it has been shown that the topological entropy of a fluid flow is an upper bound on the rate of growth of the magnetic energy [3].

The uses of the topological entropy, especially to measure the degree of chaos, provide an incentive for developing good alogorithms for calculating it. We present here a usable, effective scheme for estimating and bounding the topological entropy, h, of a piecewise monotonic map of the unit interval. In comparison to known schemes [4–6], the method is more flexible in treating maps with multiple turning points, with at least as much precision. Our method works for circle maps and can be adapted for maps on graphs. Maps with plateaus can also be treated as discussed here, but we exclude them for brevity.

Points of the interval for which a map is an extremum are called turning points, including the end points of the interval considered, and piecewise monotonic maps have a finite number of these. The locations of neighboring turning points divide the interval into segments called *laps*. For a piecewise monotonic map, f, the topological entropy is given by the exponential rate of increase with n of the monotonic upper bounds of any of these quantities: (a) the number of turning points of f^n, (b) the length of the graph of f^n, and (c) the number of periodic orbits of f^n. For such maps, these properties are equivalent [7] to the standard definitions [8].

The paradigm of piecewise monotonic maps is the family of sawtooth maps, whose slopes have constant magnitude, s, everywhere. An important special case of these is the family of tent maps

$$f_s(x)=\begin{cases} s(x-1)+2 \text{ for } 0\le x<(s-1)/s\,, \\ s(1-x) \text{ for } (s-1)/s\le x\le 1\,. \end{cases} \tag{1}$$

According to property (b), the entropy of any sawtooth map with slopes $\pm s$ is simply $\ln s$.

The central object in our method is the *topological transfer matrix*, $\mathbf{M}$. To define it, we partition the unit interval, I, by an ordered set of points $(x_0,x_1,\ldots,x_{k+1})$ so that $I=[x_0,x_{k+1}]$ is subdivided into subintervals $I_i=[x_i,x_{i+1}]$. While the subintervals I_i are not necessarily laps, some of them may contain more than one lap. We further partition such subintervals by the turning points they contain, and we let I_i^l be the lth lap contained in I_i. The elements of $\mathbf{M}$ are then defined as

$$m_{ij}=\sum_l \frac{|f(I_i^l)\cap I_j|}{|I_j|}\,, \tag{2}$$

where $|I_i|$ is the length of the interval I_i. Thus m_{ij} is the fractional amount by which $f(I_i)$, the image of I_i, covers the interval I_j, giving suitable weight to any portion that is multiply covered. Such matrices can be used in various ways; for example, in the study of invariant measures [9].

In the case of sawtooth maps on the interval [0,1] with local slopes $\pm s$, it is readily verified that the matrix $\mathbf{M}=(m_{ij})$ has the eigenvalue s, the antilog of the topological entropy, with corresponding eigenvector $(|I_0|, |I_1|,\ldots,|I_k|)^{\mathbf{T}}$. It follows directly from the Perron-Frobenius theorem [10] that this is the maximum eigenvalue.

The formula for m_{ij} is complicated because we allow for multiple covering of the target interval. We may avoid this complication by including all of the turning points of f in the partition when their number is not too large. An effective way subsequently to refine the partition to improve the accuracy is suggested by another class of maps for which the topological entropy is known exactly. These are the Markov maps, in which the orbit of every turning point is finite.

This time we choose the partition by forming an ordered set of points, $[x_0,\ldots,x_{k+1}]$, from the turning points and their orbits. Then, for each pair of subintervals, (I_i,I_j), it can be seen on constructing the partition that either $f(I_i)$ covers I_i completely or the intersection

0031-9007/93/72(1)/80(4)$06.00

of I_i with $f(I_i)$ is empty. Hence the matrix **M**, defined as before, has only 0's and 1's as entries. In this case, it is known that the entropy for the Markov map is given by the logarithm of the maximal eigenvalue of **M** [11].

For both the general Markov maps with suitable partitions and for sawtooth maps, the largest eigenvalue of **M** is the antilog of the topological entropy. These results highlight the significance of **M**. We are led to construct the topological transfer matrix for general piecewise monotonic maps by specifying suitable partitions of I. Several are possible, but one modeled after the Markov example combines accuracy with ease of construction.

Consider a piecewise monotonic map, f, whose turning points lie at the locations y_p, $p=1,2,\ldots,P$. For our partition of the interval, we now make up the ordered set of points x_i from the turning points and their images, $f^q(y_p)$, $q=0,1,2,\ldots,Q(p)-1$, counting coincident points only once. Now, at any level of refinement, we have $k=\sum_p Q(p)$ points in our partition. As we iterate each turning point in such a way that $\min_p Q(p)$ increases, the partition approximates better and better to a Markov partition. In the examples discussed below, we consider the invariant pieces of the map, and so, as in the Markov case, the limits of the interval belong to the orbits of other turning points. Hence the end points need not be treated as distinct turning points. In such cases, we take Q to be independent of p. The number of partitions is then given by $k=PQ$ where we further write $N=k-1$ and speak of the Nth level of approximation. In the exceptional case where a turning point has a finite orbit we consider only the intervals of finite length.

As in (2), we introduce the fraction by which the map of I_i covers I_j and compose the matrix with entries, m_{ij}. Once again, the entries in the matrix **M** are mostly 0's and 1's. However, in non-Markovian cases, some columns may contain subcolumns of the form $(a_{i,j},a_{i+1,j},\ldots,a_{i+m,j})^{\mathrm{T}}$ where $a_{i,l}\geq 0$ and $\sum_{k=0}^{m} a_{i+k,j}\leq 1$. The first key result is that the $\ln^+$ of the largest eigenvalue of **M** is an approximation to the topological entropy with an error that decreases with increasing N, where $\ln^+ X$ means the larger of zero and $\ln X$.

More importantly, it is also possible to put bounds on the topological entropy with this partition. To see this, we associate to the subcolumn $(a_{i,j},a_{i+1,j},\ldots,a_{i+m,j})^{\mathrm{T}}$ of **M** of length m, the m simplex, that is, the set of points $(X_0,\ldots,X_m)$ in $\mathbb{R}^{m+1}$ with $X_n\geq 0$ and $\sum X_n=1$. The extremities of this simplex are at the points $P_0=(1,0,0,\ldots,0)^{\mathrm{T}}$, $P_1=(0,1,0,\ldots,0)^{\mathrm{T}},\ldots,P_m=(0,0,0,\ldots,1)^{\mathrm{T}}$. For $m=0$, we set $P_0=0$ and $P_1=1$.

We generate a set of matrices by replacing each subcolumn $(a_{i,j},a_{i+1,j},\ldots,a_{i+m,j})^{\mathrm{T}}$ in **M** from a given lap by every possible P_n of the appropriate length, in all combinations. If we compute the largest eigenvalues of all the matrices so obtained, we get a collection of numbers whose extrema give lower and upper bounds for the largest eigenvalue of **M**, which follows in consequence of the Perron-Frobenius theorem. As can be shown from the kneading theory of Milnor and Thurston [12], these extrema give upper and lower bounds on the topological entropy, and these bounds improve when we use longer orbits of the turning points for our partitions. In certain examples, partitions may contain cells of zero length and a consistent criterion for computing m_{ij} may be needed to allow for this.

By way of illustration, we show in Fig. 1 the calculation of the entropy exponent λ, the greatest eigenvalue of **M**, for the quadratic map, $f(x)=1-ax^2$. The main panel shows the approximate value of λ for $N=2$, 3, 4, 5, and 10. The inset shows the entropy exponent for $N=10$, 15, 20, and 25 near the accumulation point of period doubling. In addition, the points marked by stars are obtained by the longer, ultimately exact calculation using

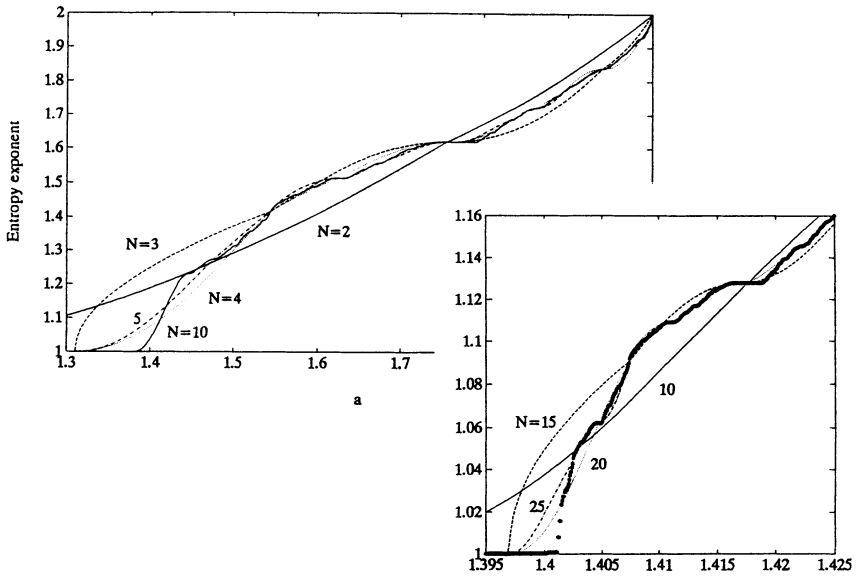

FIG. 1. The entropy exponent for the quadratic map $f(x)=1-ax^2$. The main panel shows the exponent calculated as the leading eigenvalue of the topological transfer matrix with $N=2$, 3, 4, 5, and 10. In the inset, the piece of the parameter range near the period-doubling accumulation point is shown in greater detail for calculations with $N=10$, 15, 20, and 25. The points marked by stars show the result of a calculation with kneading sequences, which would not be distinguished from the $N=10$ curve in the main panel in the parameter range outside that shown in the inset.

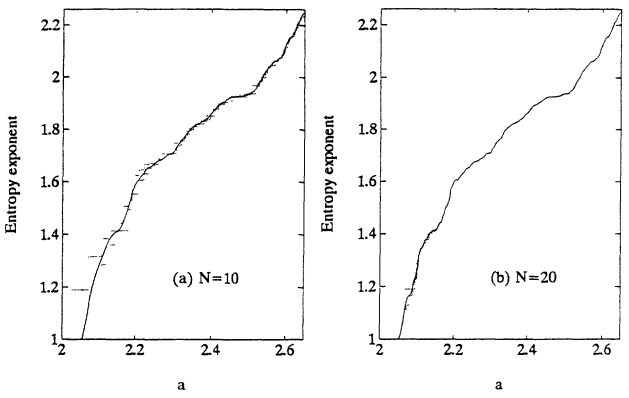

FIG. 2. The entropy exponent for the bimodal cubic map $f(x)=x^3+ax+b$ with $b=0.2$. The two panels show the approximation for the exponent (the continuous curve) and its two bounds (the dotted curves) for $N=10$ and $N=20$.

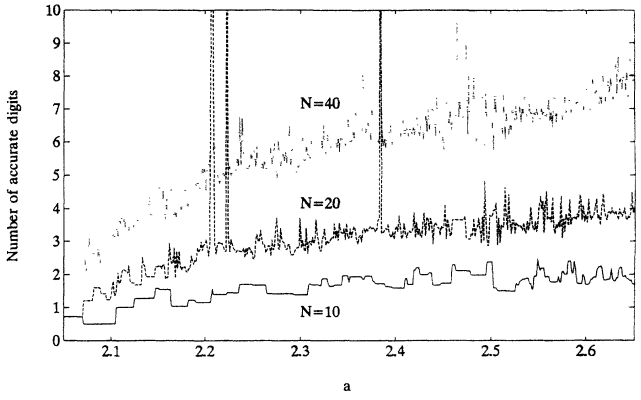

FIG. 3. The logarithm of the reciprocal of the error in the approximation as a function of a for the cubic map ($b=0.2$), estimated as the difference between the two bounds. Drawn in this way, it measures the number of digits of accuracy.

kneading sequences [4]. These are not reproduced in the main panel since they fall indistinguishably close to the calculation for $N=10$ in the parameter regime outside that drawn in more detail in the inset. For $N=2$, which for some purposes may yield the topological entropy to sufficient accuracy, we can write the largest eigenvalue simply as

$$\lambda=\begin{cases}[1+\sqrt{1+4a(1-a)^2}]/2 \text{ for } a\le a_*, \\ [\mu+\sqrt{\mu^2+4a^2(a-1)(2-a)}]/2(1-a) \text{ for } a>a_*, \end{cases} \tag{3}$$

where $\mu=a(1-a)^2+a-2$ and

$$a_*=\left[\frac{25+\sqrt{621}}{54}\right]^{1/3}+\left[\frac{25-\sqrt{621}}{54}\right]^{1/3}=1.755\ldots \tag{4}$$

is the value of a such that f has a period-three orbit containing the critical point, that is, the value of the parameter where the structure of the matrix **M** changes.

In Fig. 2, the entropy exponent is shown for the bimodal map, $f=x^3-ax+b$, for $b=0.2$ and various values of a. Results are shown for $N=10$ and $N=20$, and both the approximation and bounds are displayed for each. (Calculations for this case are also given by Bloch and Keesling [5].) The convergence properties of the method are shown in Fig. 3, which portrays the logarithm of the reciprocal of the error, estimated as the difference between the upper and lower bounds. This is equivalent to the number of digits of accuracy. In practice, the error in the largest eigenvalue of **M** is even smaller than this estimate.

For an example involving real data, we calculate the topological entropy for the empirical firing map of a stimulated marine-mollusc axon. The convergence with N is shown in Fig. 4. To construct the map $f(x)$, we fitted splines through the measurements shown in Fig. 3(d) of Hayashi *et al.* [13], and the result is shown in the inset panel of Fig. 4, together with a set of points generated by iterating the map and adding some random noise. This example illustrates the ease of calculating the topo-

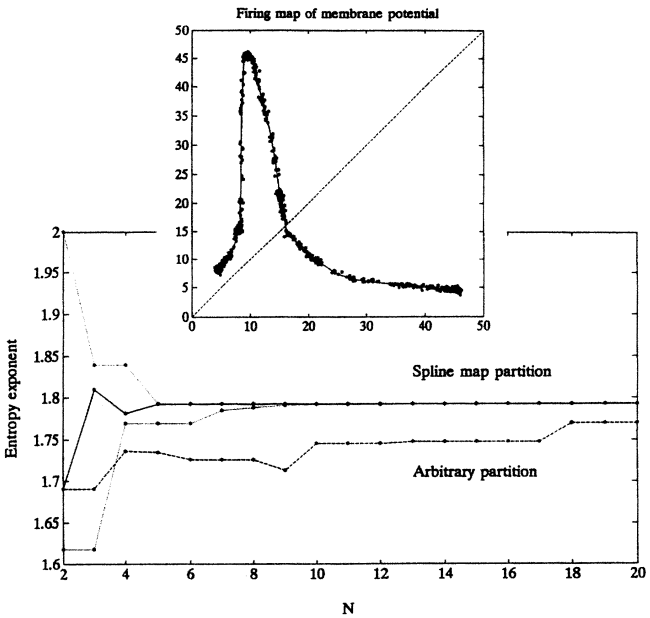

FIG. 4. The calculation of the topological entropy for the firing map of a sea-mollusc axon. The inset panel shows the map derived by fitting splines to experimental data, and also a set of points derived by iterating the map and adding random noise. The main panel shows the convergence of the calculation of the entropy exponent with N for the partition generated by iterating the critical point, and its bounds. A slowly converging calculation using an essentially arbitrary partitioning of the interval is also shown.

logical entropy if the absolute accuracy desired is not excessive; three or four iterations of the critical point are sufficient to tie the entropy down to within a few percent of its true value.

Although we advocate the use of the images of the turning points for partitions, alternative kinds of divisions could also be used. For example, if we use backward images of the turning points, rather than forward images, the matrix elements are again mostly either 0 or 1. The remaining entries are all independent of one another and, when we replace the noninteger entries by zero (or one), the largest eigenvalue of the matrix obtained is a lower (or upper) bound on the antilog of the entropy. This too follows from the Perron-Frobenius theorem and kneading theory, and makes the calculation of bounds more straightforward. In fact, the method of Góra and Boyarsky [6] is similar to this particular case of our algorithm. Unfortunately, computing preimages often requires one to solve additional equations, and the number of partitions grows rapidly as one iterates back. Such a partition rapidly becomes impractical.

Another partition can be generated by taking a set of periodic orbits each of which contains a point which lies near one of the turning points [14]. This is equivalent to approximating $f(x)$ by a Markov map, and is accurate when the orbits fall close to the turning points. However, a search is required in order to find these periodic orbits, and no bounds are given. Finally, for experimental data, uniform or measurement-determined partitions might be more accessible, although they produce relatively slow convergence (as indicated in Fig. 4 by the results of an essentially arbitrary partitioning of the firing map).

The calculation of the topological entropy of maps or flows with higher dimension is more complicated than in the one-dimensional examples considered here. There are currently no effective algorithms to compute and bound h in such situations, but property (b) above has been recently extended to smooth diffeomorphisms of n-dimensional manifolds [15]. In these cases, the topological entropy determines the growth rate of the volumes of the iterates of some submanifolds. This suggests that we might be able to generalize our method to higher dimension. For certain maps and flows, one might hope to avoid issues such as these. For example, in work to appear with G. R. Ierley we explain how to put the Hénon map and some flows in $\mathbb{R}^3$ into forms suitable for producing topological transfer matrices, though the cost in accuracy caused by conversion to one-dimensional maps has yet to be assessed.

We are very grateful to Alan Hoffman and John Milnor for helping to develop some of the proofs alluded to here. We are also indebted to Roy Adler, Viviane Baladi, Karen Brucks, Steve Childress, Bruce Kitchens, Philippe Thieullen, and Alan Wolf for comments and references. This work was supported by the AFOSR under Grant No. F49620-92-J-0061 and N.J.B. was supported by a fellowship from the SERC.

[1] R. L. Adler, A. G. Konheim, and M. H. McAndrew, Trans. Am. Math. Soc. **114**, 309 (1965).

[2] C. Tresser and P. Coullet, C. R. Acad. Sci. Paris A **287**, 577 (1978).

[3] M. Vishik (unpublished). See also J. M. Finn, J. D. Hanson, I. Kan, and E. Ott, Phys. Fluids B **3**, 1250 (1991).

[4] P. Collet, J. P. Crutchfield, and J.-P. Eckmann, Commun. Math. Phys. **88**, 257 (1983); L. Block, J. Keesling, S. Li, and K. Peterson, J. Stat. Phys. **55**, 929 (1989).

[5] L. Block and J. Keesling, J. Stat. Phys. **66**, 755 (1992).

[6] P. Góra and A. Boyarsky, Trans. Am. Math. Soc. **323**, 39 (1991).

[7] M. Misiurewicz and W. Szlenk, Studia Mathematica **67**, 45 (1980).

[8] In one standard definition [R. Bowen, Trans. Am. Math. Soc. **153**, 401 (1971)], we consider a map f from the unit cube in Euclidean space (or any compact space) to itself. A set of points in the cube is said to be $n-\epsilon$ separated if, for *each* pair of points (x,y) in the set, with $x \neq y$, there exists an m greater than zero and less than n such that $f^m(x)$ and $f^m(y)$ are separated by more than ϵ. Let $\mathcal{N}_\epsilon$ be the maximal number of points in any set that is $n-\epsilon$ separated. For fixed ϵ we let n go to infinity and look at the rate of increase of the monotonic upper bound of $\mathcal{N}_\epsilon$ with n. The limit of this rate as $\epsilon \to 0$ is the topological entropy of f.

[9] F. C. Hoppensteadt, *Analysis and Simulation of Chaotic Systems* (Springer-Verlag, Berlin, 1993).

[10] W. F. Gantmacher, *Theory of Matrices* (Chelsea, New York, 1959), Vol. 1.

[11] See, for example, C. S. Hsu and M. C. Kim, Phys. Rev. A **31**, 3253 (1985).

[12] J. Milnor and W. Thurston, in *Dynamical Systems*, edited by James C. Alexander, Lecture Notes in Mathematics Vol. 1342 (Springer, Berlin, 1988), p. 465.

[13] H. Hayashi, S. Ishizuka, M. Ohta, and K. Hirokawa, Phys. Lett. **88A**, 435 (1982).

[14] L. Bloch and E. Coven, in *Dynamical Systems and Ergodic Theory* (Polish Sci. Publishers, Warsaw, 1989), p. 237.

[15] S. E. Newhouse, Ergod. Th. Dynam. Syst. **8**, 283 (1988); Y. Yomdin, Israel J. Math. **57**, 285 (1980); **57**, 301 (1980).